Effect of deviation from stoichiometry and thermal annealing on amorphous gallium antimonide films

J. H. Dias da Silva* and J. I. Cisneros
Instituto de Física "Gleb Wataghin," Universidade Estadual de Campinas, CP 6165, CEP 13081-970, Campinas, São Paulo, Brazil

M. M. Guraya and G. Zampieri
Comisión Nacional de Energia Atómica, Centro Atómico Bariloche e Instituto Balseiro, 8400 Bariloche, Argentina
(Received 3 June 1994; revised manuscript received 29 November 1994)

a-$Ga_{1-x}Sb_x$ films were deposited in a specially designed flash evaporation apparatus. The control of the evaporation parameters allowed us to prepare stoichiometric and Sb-rich samples. The physical properties of the material were analyzed using optical spectroscopy, x-ray diffraction, electrical conductivity, Raman scattering, infrared absorption, electron energy loss, and Auger electron spectroscopies. The dark conductivity of several samples of variable composition was measured. Variable range hopping dominates the transport process for stoichiometric material while in the Sb-richer samples the phonon-assisted hopping between tail states probably dominates. A substantial increase in the electrical conductivity due to chemical disorder is observed when the composition is far from stoichiometry. A sequence of heat treatments of a near-stoichiometric sample showed two qualitatively different effects. At low temperatures, before the onset of crystallization, an ordering of the amorphous matrix is observed. At higher annealing temperatures GaSb and Sb crystallites are formed. The experimental data and current theories suggest that the partially crystallized material is a mixture of stoichiometric GaSb (and eventually Sb) microcrystals embedded in an Sb-rich a-$Ga_{1-x}Sb_x$ matrix. The effects of disorder produced by the departure from stoichiometry and by partial crystallization were compared.

I. INTRODUCTION

Amorphous III-V semiconductor compounds have optical and electrical properties that indicate them as strong candidates for the development of several kinds of electrical and optical devices. However the nature of the defect states in these materials is not yet completely understood,[1-4] so that their control is difficult if not impossible at the present time. In these materials, in addition to the structural disorder, common to all amorphous solids, we have to include chemical disorder, which prevents the direct comparison between their properties and those of the well-known elemental semiconductors a-Si and a-Ge.

In spite of the fact that little research on III-V amorphous semiconductors has been done up to now, some basic properties are well established.[5-8] The local order with tetrahedral coordination is maintained as in amorphous silicon and germanium.[5,9] Stoichiometry is difficult to attain in the preparation of these materials. The methods most frequently used to overcome this difficulty are flash evaporation[10-12] and sputtering.[3,13] Usually the column-V element is in excess. Previous studies, however, indicate that the excess element atoms are uniformly distributed in the matrix, resulting in homogeneous amorphous solids.[5,6,14,15]

Detailed theoretical calculations of the electronic structure of the III-V amorphous semiconductors, including the defect states, were performed by O'Reilly and Robertson.[1] A tight-binding recursion method was used. They proposed that the main kind of defect in these materials should be threefold-coordinated atoms, essentially because most of the column-III and column-V elements are trivalent. In this way the dangling-bond sites are expected to relax to configurations very similar to those found in the relaxed surface of c-GaAs: the As dangling bond relaxes from the bond angle of 109.5° towards 97° when its level is filled. Similarly, the Ga dangling bond relaxes towards 120° as its level empties. A consequence of this relaxation is that the diamagnetic configurations are much more probable than the half-filled dangling-bond configurations in GaAs and the other III-V amorphous compounds. Besides, these relaxed dangling-bond sites (called here C_3 sites) are expected at energy levels near the band edges or inside the bands, instead of giving deep gap states.

According to the O'Reilly and Robertson model, wrong bonds (bonds between like atoms) cause gap states in some of the III-V compounds. The III-III wrong bond generally produces acceptor states while V-V wrong bonds are expected to produce donor states. The formation energies of these defects are higher than those necessary to form the others and consequently the density of wrong bonds should be smaller than the C_3 density.

Hydrogenation, a fundamental process for the control of defect states in a-Si, has been attempted in a-GaAs (Refs. 13,16) and a-GaP.[17,18] In spite of the clear improvements of the electronic properties induced by this process, the role of hydrogen is not well understood. The different nature of the chemical bonds in a-Si and III-V compounds makes the understanding of the passivation of dangling bonds difficult.

Structural studies indicate that different kinds of defects are present in these compounds, mainly changes in the predominant tetrahedral coordination and, to some

extent, wrong bonds, i.e., bonds between like atoms. The low energy necessary for breaking the wrong bonds[15] suggests that thermal annealing can be used to reduce the density of at least this kind of defect. In fact, changes in the optical and structural properties of these materials have already been observed when treated at even low temperatures.[11,19,20]

In this work we mainly study the optical properties of amorphous gallium antimonide films prepared by flash evaporation. The effect of stoichiometry deviations and heat treatments on the optical absorption edge was studied using optical transmission data. The crystallization process was followed by means of x-ray diffraction, Raman scattering, and optical reflectivity in both uv and ir bands. The electrical conductivity was measured as a function of Sb concentration in stoichiometrically unbalanced samples as well. The composition of the samples was determined by means of x-ray photoelectron (XPS) and Auger electron spectroscopies (AES).

The similarities between the changes in the absorption edge produced by crystallization in nearly stoichiometric samples and those corresponding to unbalanced materials with different Sb concentrations are analyzed.

II. EXPERIMENTAL PROCEDURE

A set of a-$Ga_{1-x}Sb_x$ films with different concentrations ($0.50 < x < 0.59$) and thicknesses ranging from 200 to 1200 nm were deposited onto silica glass and crystalline silicon substrates using the flash evaporation technique,[10,11,21] in a specially designed equipment described elsewhere.[22] The evaporation assembly is basically composed of a high-vacuum chamber with a feeder, a crucible, and a substrate holder. The feeder is able to continuously supply the hot crucible with crystalline GaSb powder. The feeding rate of 0.3 g/min adopted in this work resulted in deposition rates of approximately 3 nm/s. The source material was a GaSb powder, made from a pure single crystalline rod, with a mean grain size of 30 μm. The relevant properties of the source material were a carrier concentration of 1.5×10^{17} cm^{-3}, electrical conductivity of 13.9 Ω^{-1} cm^{-1}, and p-type character due to native defects. The substrates were kept at room temperature during the depositions.

The crucible temperature T_c was used to control the composition of the material. Stoichiometric and near-stoichiometric samples were prepared at high temperatures (1040–1070 °C). Large Sb excesses were obtained at lower temperatures. The higher limit of T_c was set at 1200 °C because at higher values pinholes appear in the films due to collision of solid GaSb particles coming from the crucible. Samples prepared at temperatures higher than this limit show some crystallization as well.

Standard evaporation was used in the deposition of a few samples. The properties of these and of the flash evaporated ones were compared.

Table I contains the crucible temperature, composition, and optical parameters of a representative group of samples.

XPS, AES, and energy loss measurements were performed in an ultrahigh-vacuum (UHV) chamber with a base pressure of 10^{-10} Torr. The Auger spectra of the samples as introduced into the UHV chamber showed O-KVV signals, typical of air-exposed samples, which disappeared completely after a mild Ar sputtering. We paid special attention to the presence of W, finding that the samples were completely free of this contaminant. For the XPS measurements we used Al K radiation and we determined the compositions from the intensity ratios of the Ga 3d and Sb 4d peaks.

TABLE I. Crucible temperatures (T_c), Sb concentration (X), optical gaps (E_g), Urbach energies (E_0), and Wemple and DiDomenico parameters (E_m,E_d) of a-$Ga_{1-x}Sb_x$ films.

T_c (°C)	x	E_g (eV)	E_0 (meV)	E_m (eV)	E_d (eV)
1070	0.50	0.58	152	1.6	30±4
1070	0.51	0.53	196	1.9	33±3
1040	0.52	0.49	227	2.0	40±4
990	0.59		344	1.6	39±5

The energy loss spectra of 1 keV electrons were previously measured,[23] showing peaks at approximately 14 eV attributed to the excitation of bulk plasmons. The position and width of these peaks did not undergo important changes with composition.

Transmittance and reflectance spectra at normal incidence were measured in different spectrophotometers: Perkin Elmer Lambda 9 from 6.2 to 0.5 eV, Jasco IR 700 from 4000 to 400 cm^{-1}, and BIO-RAD FTS 40 from 400 to 190 cm^{-1}. This wide range encloses the main features of the optical spectra of GaSb, the maximum of the imaginary part of the dielectric function being found at 2.5 eV,[8] while at the ir side one cold measure a phonon absorption band at 225 cm^{-1}.

The Raman spectra were measured at room temperature using the emission line of an argon laser at 514.5 nm. Low excitation intensities were adopted in order to prevent laser annealing of the samples.

The dark electrical conductivity was measured in a high-vacuum chamber (7×10^{-4} Pa) as a function of the temperature in the range 150–423 K. The electrical contacts were aluminum parallel strips deposited on the substrates' surfaces before the film growth in order to prevent contamination effects at the film surface. The experimentally determined positive signal of the Seebeck factor indicated p-type electrical conduction in all the samples.

The refractive index, the absorption coefficient, the Urbach energy E_0, the Tauc optical gap E_g,[24] and the film thickness were determined using transmittance and reflectance data measured at room temperature. Analytical expressions for the transmittance and reflectance of a thin film on a weakly absorbing thick substrate were used in the calculations. Multiple reflections, coherent in the film and incoherent in the substrate, were considered in the derivation of these formulas.[25,26]

The calculations of the optical constants were performed in two steps. In the first one, data from the low-absorption region, with clear interference fringes, were used. Wemple and DiDomenico (WD) parametrization

of the refractive index [Eq. (1) below] and the Urbach formula for the absorption coefficient [Eq. (2) below] were adopted to fit the transmittance and reflectance spectra simultaneously:

$$n(\hbar\omega)=\left[1+\frac{E_m E_d}{E_m^2-(\hbar\omega)^2}\right]^{1/2}, \quad (1)$$

$$\alpha(\hbar\omega)=\alpha_0 e^{\hbar\omega/E_0}. \quad (2)$$

E_m and E_d are the oscillator and dispersion energies, respectively, α_0 is the pre-exponential absorption factor, and E_0 is the Urbach energy.

The second step of the optical calculation uses transmission data at the absorption edge region (low transmission values) which are very sensitive to the variations of α. An efficient iterative procedure,[25] which makes use of the refractive index and the film thickness of the previous step, was adopted in this case.

The results more relevant to this work are the absorption coefficient at the absorption edge, the optical gap E_g, and the Urbach energy E_0. It should be recalled that, according to Cody *et al.*,[27] E_0 is directly related to the disorder of the material. In amorphous compound semiconductors we consider three additive contributions to the Urbach energy: (i) a thermal or phonon term E_{0T}, (ii) a term related to topological disorder and defects common to all amorphous solids E_{0a}, and (iii) a term associated with chemical disorder E_{0ch}, which only appears in compound solids. As the measurement temperature was not varied in our experiments, E_{0T} is a constant.

III. RESULTS

The absorption edges of the materials with different Sb concentrations (x) are shown in Fig. 1(a). The Urbach energy E_0 increases with x, Fig. 1(b), reflecting the growing of disorder. The optical gap, determined according to Tauc's method,[24] narrows as the Sb concentration increase. Figure 1(c) shows this feature; it can also be observed that the steepness of the straight lines of the unbalanced samples is less than that of the stoichiometric sample, leading to a crossing of the Tauc plots corresponding to $x=0.50$ and 0.51.

The properties of the material evaporated by the standard procedure change during the deposition, as expected. Samples obtained at the beginning of the evaporation have properties similar to those of the flash evaporated ones. At later evaporation times, the properties of the corresponding samples change rapidly as the Sb concentration increases. In this condition the absorption edge becomes less defined [sample SE in Fig. 1(a)] and finally the film is mechanically unstable, detaching easily from the substrate.

The dark electrical conductivity was measured as a function of T for various compositions [Figs. 2(a) and 2(b)]. No irreversible changes of the physical properties of the materials were detected after these measurements, in which the maximum temperature achieved was 435 K.

The conductivity vs inverse temperature plots [Fig. 2(a)], are not exponential, not allowing an unambiguous determination of the activation energy which would characterize free-carrier conduction. The analyzed materials have rather different optical gaps and conductivities, and indeed the two extreme compositions ($x=0.50$ and 0.59) should be associated with very different materials, whose energy bands are significantly different.

In the stoichiometric sample, $x=0.50$, the one with the lowest density of gap states, the conductivity vs $1/T$ behavior might be interpreted as being due to free carriers if a statistical shift of the Fermi energy as a function of the temperature occurred during the measurement. Nevertheless, its strong $T^{-1/4}$ behavior [Fig. 2(b)] indicates that variable range hopping is the more probable conduction mechanism.

The sample with $x=0.59$, the most unbalanced one, shows a high conductivity which is almost independent of temperature, a very narrow optical gap, and a broad Urbach tail. The density of states at the Fermi level should be very high, and hopping between these tail states are very probable.

The conductivity of the materials with intermediate compositions, $x=0.51$ and 0.52, increases with the Sb concentration but its behavior with temperature cannot be explained any longer by variable range hopping. Probably the increase of the density of states in the band tails and in the gap favors phonon-assisted hopping between near neighbors.

In order to study eventual structural changes and the crystallization of the material, a sequence of thermal annealings ($T_a=180$, 210, 250, and 400 °C, and $t_a=20$ min) was performed. A nitrogen atmosphere was used to prevent surface oxidation. After each treatment the following spectra were measured: x-ray diffraction, optical reflection in the ultraviolet/visible region, transmittance at the absorption edge, transmittance and reflectance in the infrared, and Raman scattering. In Figs. 3–6 we show the evolution of the spectra of a nearly stoichiometric sample ($x=0.51$). The spectrum of the as-grown sample was included in each case.

Figure 3(a) shows that no peak in the x-ray diffraction spectrum is observed after the first annealing ($T_a=180$ °C). The beginning of crystallization is clearly seen after the annealing at 210 °C, where the emerging peaks correspond in angular position and intensity ratios to those of crystalline GaSb. The annealings at the higher temperatures, 250 and 400 °C, produced a strong increase in peak intensity and a somewhat weak peak narrowing. The mean size of the GaSb crystallites, related to the peak width and given by the Scherrer formula,[28] varies from 220±20 Å for the lower T to 270±20 Å for the highest one (400 °C). Two peaks at $2\theta=28.8°$ and 40.1°, associated with c-Sb, are observed after the annealing at 400 °C.

The evolution of the imaginary part of the dielectric function ε_2 [Fig. 3(b)] determined using a multiple-oscillator fitting of the reflectance data follows a trend quite similar to that of the x-ray diffraction. Peaks in ε_2 begin to appear at $T_a=210$ °C, indicating the onset of singularities in the density of electronic states, proper to the crystalline phase. As the annealing temperature increases the ε_2 spectra become closer and closer to that of

the crystalline GaSb sample. The optical gaps and Urbach energies of the as-grown and heat-treated a-$Ga_{0.49}Sb_{0.51}$ samples are plotted in Figs. 4(a) and 4(b), respectively. It should be observed that the annealing at 180 °C, which did not produce any appreciable change either in the x-ray diffractogram or in the ε_2 spectrum, induced a clear opening of the optical gap accompanied by a diminution of the Urbach energy. A contrary effect is produced by the annealings at higher temperatures.

Raman scattering and ir absorption experiments were performed in order to get information about eventual structural ordering of the lattice at the lowest annealing temperature (180 °C) as suggested by the opening of the gap seen in Fig. 4(a). The sequence of Raman scattering spectra is shown in Fig. 5. The peaks at 226 and 235 cm^{-1} correspond to the TO and LO vibrational modes of GaSb, respectively. The peak at 152 cm^{-1}, which appears in the 400 °C annealing, is attributed to c-Sb,[29] be-

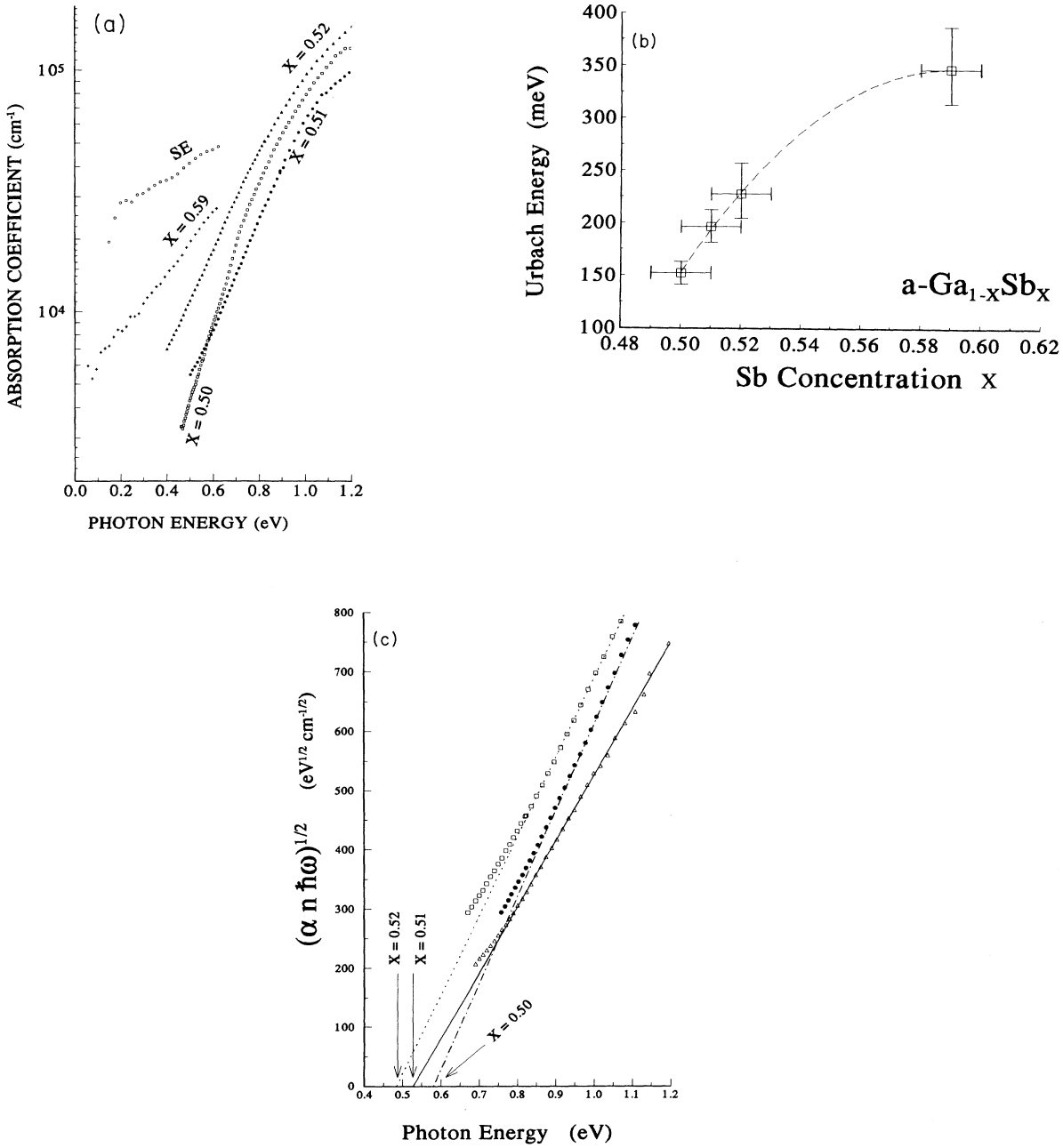

FIG. 1. Optical absorption of a-$Ga_{1-x}Sb_x$ films of different concentrations. (a) Absorption edges, (b) Urbach energies E_0, and (c) Tauc plots used to determine the optical gaps. The absorption edge labeled SE in (a) corresponds to a sample prepared at later times in a standard evaporation.

ing specially suited to detect Sb clusters due to its high scattering cross section. The reflectance spectra at the restrahlung phonon region are shown in Fig. 6. Both ir and Raman spectra taken after the annealing at 180 °C reveal features related to structural modifications, not ob-

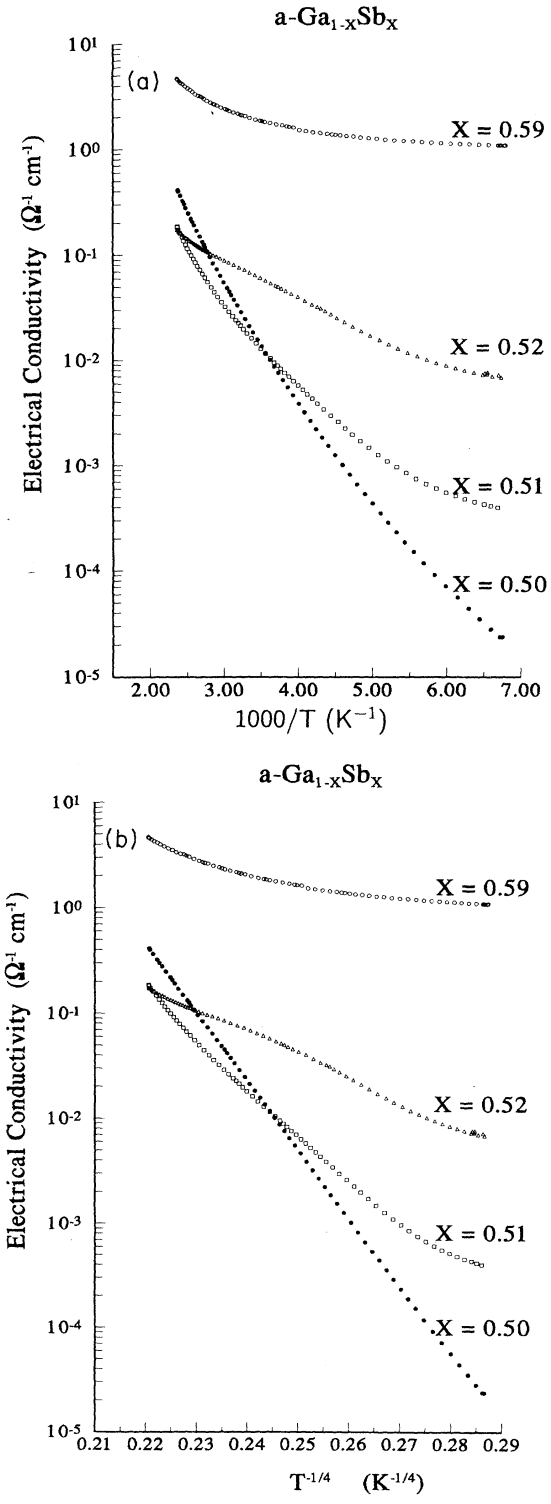

FIG. 2. Dark electrical conductivity of a-$Ga_{1-x}Sb_x$. (a) Conductivity vs $1000/T$ and (b) conductivity vs $T^{-1/4}$.

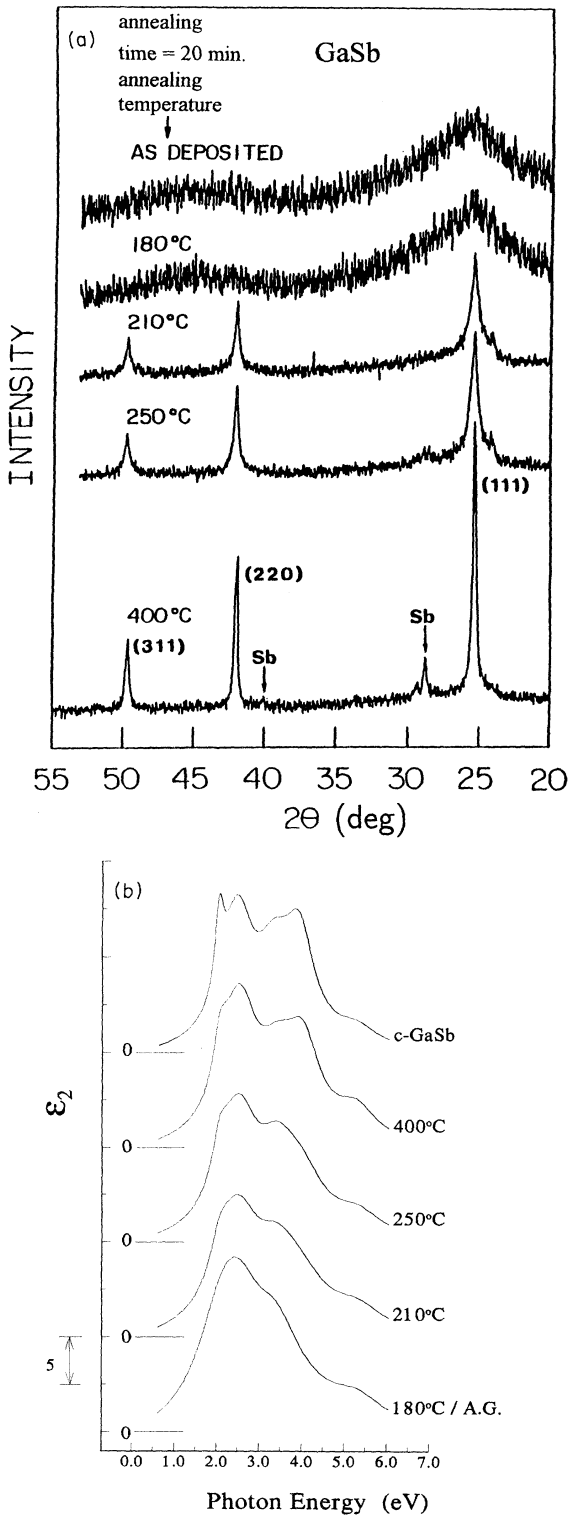

FIG. 3. (a) X-ray diffraction patterns of an a-$Ga_{0.49}Sb_{0.51}$ film thermally annealed at different temperatures. (b) Imaginary part of the dielectric function vs photon energy for an a-$Ga_{0.49}Sb_{0.51}$ film. The spectra correspond to multiple-oscillator fittings of reflectance data for different annealing temperatures. The spectrum of the as-grown (AG) film and that corresponding to an annealing at 180 °C are identical. The results of a polished GaSb slab were included for comparison.

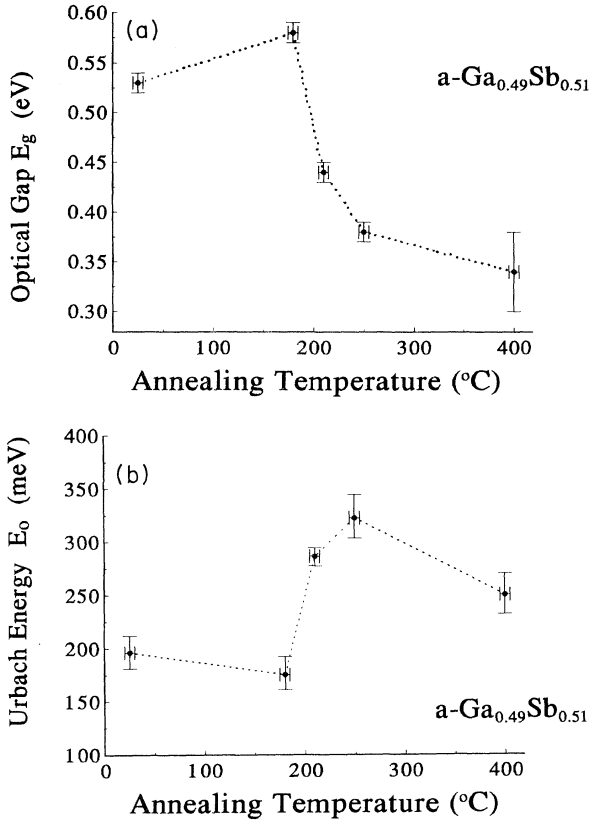

FIG. 4. Optical gap (a) and Urbach energy (b) of a-$Ga_{0.49}Sb_{0.51}$ as functions of the annealing temperature.

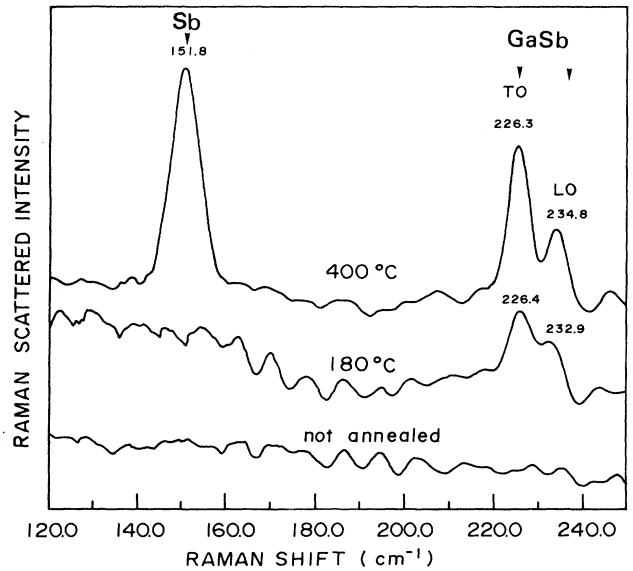

FIG. 5. Raman scattered intensity vs excitation line shift (514.5 nm argon laser) in an a-$Ga_{0.49}Sb_{0.51}$ film on a silicon substrate, annealed at different temperatures. The 180 °C spectrum shows a peak structure associated with the TO and LO vibrational modes of c-GaSb. These peaks become well defined in the 400 °C annealing. The intense peak at 151.8 cm^{-1} found in this annealing is associated with the formation of pure Sb crystallites.

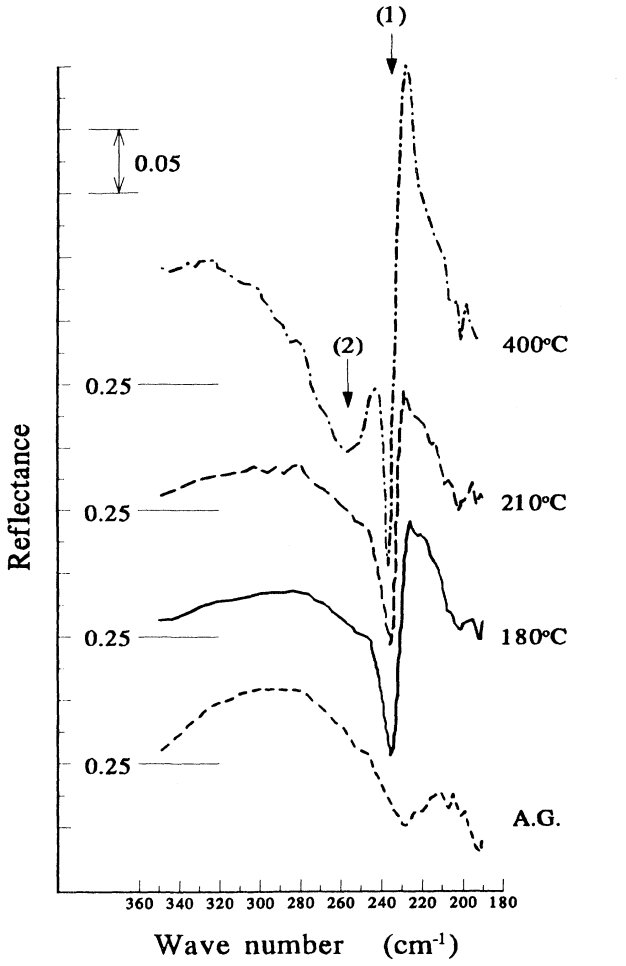

FIG. 6. Reflectance spectrum of an a-$Ga_{0.49}Sb_{0.51}$ film on a silicon substrate submitted to a sequence of thermal annealings. The band at 230 cm^{-1} (1) corresponds to the reststrahlung phonon excitation in c-GaSb. Observe that the spectrum for the 180 °C annealing is qualitatively different from that for the as-grown film (AG). The large band (2) is probably related to the formation of Sb crystallites.

served in the x-ray and reflection data, which will be discussed in the next section.

IV. DISCUSSION

It is shown that the absorption spectra of near-stoichiometric a-GaSb materials are characterized by a well-defined Urbach tail and a sublinear region at higher energies, characteristic of a homogeneous semiconductor compound, as might be expected according to previous works.[5,6,14,15] As the Sb concentration increases ($x > 0.50$), the Urbach energy increases and the optical gap becomes narrower.

Theoretical studies of the electronic properties of

amorphous III-V semiconductors suggest C_3 centers (threefold-coordinated atoms) and wrong-bond complexes, respectively, as the defects responsible for the formation of band tails and deep states in the gap.[1,2] According to these studies the isolated C_3 levels are at -0.45 eV for Sb sites, and $+1.37$ eV for the Ga sites (both energies referred to the valence-band top of a-GaSb whose energy gap is 0.78 eV). The energies of these sites may be significantly shifted by the influence of their environments. For instance, in the extreme case of two adjacent Sb C_3 sites, the energy goes to $+0.50$ eV. Intermediate distances between C_3 sites give a distribution of states which could contribute to the tails. Thus C_3 and wrong-bond defects plus the distorted bonds of tetracoordinated atoms determine the density of gap states in these materials.

In near-stoichiometric a-$Ga_{1-x}Sb_x$ the density of wrong bonds should be low because of the strong tendency to chemical ordering, which promotes a well-defined absorption edge with tails dominated by the C_3 defect centers. However, in off-stoichiometric material we should expect to some extent higher densities of wrong bonds in addition to the C_3 centers. The great increase of optical absorption, especially at low energies, in our strongly unbalanced samples (a-$Ga_{0.41}Sb_{0.59}$ and sample SE) is consistent with this explanation.

The global increase of the electrical conductivity as a function of x is due to the growth of the density of band tail and gap states, related to the growing chemical disorder. The stoichiometric material has small defect density, mainly Sb C_3 centers, this being the only case in which the transport is clearly dominated by variable range hopping. Materials with increasing Sb concentration do not show linearity of $\log\sigma$ with either $T^{-1/4}$ or T^{-1}; this behavior indicates that thermally activated hopping between near-neighbor tail states grows in importance as x increases.

The signal of the Seebeck factor measured at room temperature indicates that in all cases our material has p-type electrical conductivity. This result is also consistent with the theoretical models mentioned above: the Sb C_3 centers create acceptor states that dominate the conductivity process once the material is richer in Sb. In this case the probability for the formation of Ga C_3 centers is small, resulting in a low density of donor states. However, the applicability of the O'Reilly and Robertson model to the prediction of the signal of the Seebeck factor is inconclusive in the case of samples with high Sb excess, where Sb-Sb wrong bonds are highly probable, thus creating donor states as well.

The effects of the low-temperature heat treatment (180 °C), were detected by means of ir and Raman measurements and by the alteration of the absorption edge as well. Probably during this first annealing, which did not induce any detectable crystallization, a number of defects (distorted and wrong bonds) were eliminated. This local reorganization of the matrix should be responsible for the observed decrease of the Urbach energy (Table I) and the opening of the gap. At this stage migration of Sb atoms probably did not occur, so the decrease in E_0 is not influenced by a variation of E_{0ch}. The broad ir absorption band (Fig. 6) of the as-grown sample becomes narrower and more intense after the first annealing, reflecting the less damped oscillations of the more ordered material.

The crystallization of the almost stoichiometric material produced by the higher-temperature annealings is clearly demonstrated by the x-ray data. The crystallites thus formed should be strictly stoichiometric[30] as compared to the originally amorphous matrix. This means that some antimony should be ejected out of the crystallized regions to the still amorphous matrix in its vicinities, increasing its Sb concentration. Such treated material is then a mixture of small stoichiometric crystals and a stoichiometrically unbalanced amorphous matrix, and should share the properties of both phases. At the highest annealing temperature Sb segregation and crystallization occur and are observed by means of the x-ray diffraction patterns and Raman scattering experiments that show the characteristic peaks of antimony [Figs. 3(a) and 5].

It should be noted that in this mixture of crystalline and amorphous phases the grain boundaries are regions of high density of defects that, according to the above theoretical models, should be predominantly Sb C_3 centers.

In the spectral region where the optical absorption of the amorphous phase is high, the optical behavior of an originally unbalanced amorphous sample and a partially crystallized heat-treated one should be comparable in some way. In Fig. 1(b) we have plotted the Urbach energy as a function of the Sb concentration x of the stoichiometrically unbalanced samples (not heat treated), and in Fig. 4(b), the E_0 values of a single heat-treated sample were plotted as a function of the annealing temperature. Comparing these figures, the following points should be noted. (i) E_0 is a monotonically increasing function of x in the off-stoichiometric (not heat-treated) samples [Fig. 1(b)]. (ii) The ranges of variation of E_0 in both plots 1(b) and 4(b) are similar. The smaller values of E_0 [4(b)] before crystallization are comparable to the ones of the nearly stoichiometric samples in Fig. 1(a). Similarly, highly unbalanced samples have E_0 values comparable to those of the crystallized samples. (iii) Figure 4(b) shows a strong increase in E_0 (210 and 250 °C) and then a decrease (400 °C); these features are coherent with the initial Sb migration and incorporation in the amorphous phase (greater chemical disorder) occurring during the annealings at 210 and 250 °C. The segregation and crystallization of Sb induced by the highest-temperature annealing reduce the Sb concentration in the amorphous phase and concomitantly reduce the chemical disorder.

The previous discussions demonstrate that the structure of the partially crystallized material is composed of stoichiometric GaSb (and eventually Sb) microcrystals, embedded in an amorphous matrix with Sb excess. We show, in addition, that this amorphous matrix has the same properties as the highly unbalanced amorphous material studied separately. X-ray diffraction experiments were able to probe the crystallinity of this composite material while the optical techniques gave information about

the amorphous phase.

ACKNOWLEDGMENTS

We wish to thank Dr. M. M. G. de Carvalho and C. E. M. de Oliveira for preparing the GaSb rods, Dr. L. P. Cardoso for the x-ray diffraction measurements, Dr. J. C. Galzerani for the Raman scattering spectra, and Dr. F. Alvarez for discussions on the transport mechanisms. The work was partially supported by Fapesp and CNPq (Brazil) and Conicet (Argentina).

*Permanent address: Depto. de Física, Fac. de Ciências, UNESP, CP 473, CEP 17033-360, Bauru-SP, Brazil.

[1]E. P. O'Reilly and J. Robertson, Phys. Rev. B **34**, 8684 (1986).

[2]E. Fois, A. Selloni, G. Pastore, Q. M. Zhang, and R. Car, Phys. Rev. B **45**, 13 378 (1992).

[3]A. Deville, B. Gaillard, K. Sedeek, H. Carchano, and K. W. H. Stevens, J. Phys. Condens. Matter **1**, 9369 (1989).

[4]G. Edelin and D. Mathiot, Philos. Mag. B **42**, 95 (1980).

[5]N. J. Shevchik and W. Paul, Non-Cryst. Solids **13**, 1 (1974).

[6]J. Dixmier, A. Gheorghiu, and M. L. Thèye, J. Phys. C **17**, 2271 (1984).

[7]A. Gheorghiu and M. L. Thèye, J. Non-Cryst. Solids **35/36**, 397 (1980).

[8]J. Stuke and G. Zimmerer, Phys. Status Solidi B **49**, 513 (1972).

[9]M. L. Thèye, A. Gheorghiu, K. Driss-Khodja, and C. Boccara, J. Non-Cryst. Solids **77&78**, 1293 (1985).

[10]W. Eckenbach, W. Fuhs, and J. Stuke, J. Non-Cryst. Solids **5**, 264 (1971).

[11]A. Gheorghiu, T. Rappeneau, S. Fisson, and M.-L. Thèye, Thin Solid Films **120**, 191 (1984).

[12]A. Gheorghiu, T. Rappeneau, J. P. Dupin, and M. L. Thèye, J. Phys. (Paris) Colloq. **42**, C4-881 (1981).

[13]W. Paul, T. D. Moustakas, D. A. Anderson, and E. Freeman, in *Proceedings of the 7th International Conference of Amorphous and Liquid Semiconductors, Edinburgh, 1977,* edited by W. E. Spear (Centre for Industrial Consultancy and Liaison, University of Edinburgh, Edinburgh, 1977), pp. 467–471.

[14]D. Udron, A. M. Flank, A. Gheorghiu, P. Lagarde, and M. L. Thèye, Philos. Mag. Lett. **59**, 9 (1989).

[15]N. J. Shevchik and W. Paul, J. Non-Cryst. Solids **16**, 55 (1974).

[16]D. K. Paul, J. Blake, S. Oguz, and W. Paul, J. Non-Cryst. Solids **35/36**, 501 (1986).

[17]H. Kubota and M. Onuki, J. Non-Cryst. Solids **115**, 39 (1989).

[18]M. Onuki, T. Fujii, and H. Kubota, J. Non-Cryst. Solids **114**, 792 (1989).

[19]V. N. Denisov, B. N. Mavrin, V. B. Podobedov, and G. G. Skrotskaya, JETP Lett. **50**, 393 (1989).

[20]B. S. Naidu, A. K. Sharma, D. V. K. Sastry, Y. Syamalamba, P. Jayarama Reddy, J. Non-Cryst. Solids **42**, 637 (1980).

[21]L. Harris and B. M. Siegel, J. Appl. Phys. **49**, 734 (1948).

[22]J. H. Dias da Silva, J. I. Cisneros, and L. P. Cardoso, in *Crystallization and Related Phenomena in Amorphous Materials–Ceramics, Metals, Polymers, and Semiconductors,* edited by M. Libera, T. E. Haynes, P. Cebe, and J. Dickinson, MRS Symposia Proceedings No. 321 (Materials Research Society, Pittsburgh, 1994), pp. 645–650.

[23]J. H. Dias da Silva, J. I. Cisneros, C. E. M. de Oliveira, M. M. Guraya, and G. Zampieri, J. Phys. Condens. Matter **5**, A343 (1993).

[24]J. Tauc, in *Optical Properties of Solids,* edited by F. Abeles (North-Holland, Amsterdam, 1972), Chap. 5, pp. 279–313.

[25]J. H. Dias da Silva, J. I. Cisneros, M. P. Cantão, and F. C. Marques, in *Current Topics on Semiconductor Physics,* edited by O. Hipolito, A. Fazzio, and G. E. Marques (World Scientific, Singapore, 1988), pp. 192–197.

[26]J. I. Cisneros, G. B. Rego, M. Tomyiama, S. Bilac, J. M. Goncalves, A. E. Rodrigues, and Z. P. Arguello, Thin Solid Films **100**, 155 (1983).

[27]G. D. Cody, T. Tiedje, B. Abeles, B. Brooks, and Y. Goldstein, Phys. Rev. Lett. **47**, 1480 (1981).

[28]See, for instance, L. V. Azároff, *Elements of X-Ray Crystallography* (McGraw-Hill, New York, 1968), p. 552.

[29]R. Carles, J. B. Renucci, A. Gheorghiu, and M. L. Thèye, Philos. Mag. B **49**, 63 (1984).

[30]D. Weiler and H. Mehrer, Philos. Mag. A **49**, 309 (1984).